J Syst Sci Complex (2016) XX: 1–23

Time-variant Consensus Tracking Control for Networked Planar Multi-agent Systems with Non-holonomic Constraint*

ZHAO Jun · LIU Guo-Ping

DOI:
Received: Oct. 20 2016 / Revised: Jan. 28 2017

Abstract A time-variant consensus tracking control problem for networked planar multi-agent systems with non-holonomic constraints is investigated in this paper. In the time-variant consensus tracking problem, a leader agent is expected to track a desired reference input, simultaneously, follower agents are expected to maintain a time-variant formation. To solve the time-variant consensus tracking problem of planar multi-agent systems with non-holonomic constraints, a time-variant consensus tracking control strategy is designed on the basis of a unidirectional topology structure. One of main contributions of this paper is the time-variant consensus tracking protocol for general time-variant formations of planar multi-agent systems with non-holonomic constraints, the other main contribution of this paper is an acitve predictive control strategy, where predictions of agents are generated acitvely, so that the computational efficiency is improved than passive approaches. The proposed control strategy is verified by two types of time-varying formations of wheeled mobile robots, and the experimental results show that the proposed control strategy is effective for general time-variant consensus tracking problems of planar multi-agent systems with non-holonomic constraints in local and worldwide networked environments.

Keywords Networked multi-agent system, networked predictive control, non-holonomic constraint, time-variant consensus, consensus tracking.

1 Introduction

A time-variant consensus tracking control problem for planar multi-agent systems with non-holonomic constraints has been discussed in this note. The "consensus tracking" problem[1] is

Center for Control Theory and Guidance Technology, Harbin Institute of Technology, Harbin, 150080, China. E-mail :zjlzl1031@icloud.com; School of Engineering, University of South Wales, Pontypriid CF371DL, United Kindom. E-mail :guoping.liu@southwales.ac.uk

*This research was supported by National Natural Science Foundation of China under Grant No.61333033 and 61690212.

◇ *This paper was recommended for publication by Editor .*

widely discussed. Based on Ref [1], the discussion of "consensus tracking" is expended on event-trigged approaches [2], linear systems under networked observability conditions [3], adaptive consensus approaches [4], linear systems with switching topology structures [5], systems with measurement noises [6], robust control approaches [7] etc. Mentioned problems can be classified into two categories: (1) States of agents are expected to be consistent, where a leader agent is assumed as autonomous (an agent without control input) with known dynamics; (2) States of the follower agents are expected to trend a desired state consistently. Generally, on the both problems, agents are expected to track a desired object consistently. Hence, in the "consensus tracking" problems, the objects of consensus and tracking are equivalent, i.e. the consensus is reached as long as all agents track the desired position. However, the time-variant consensus tracking control problem discussed in this note is different from ones in mentioned literatures. The time-variant consensus tracking control discussed in this note is expressed as follows: a leader agent is expected to track a desired time-variant reference input, simultaneously, follower agents are expected to maintain desired time-variant relationships with the leader agent. In this approach, the reference input is not necessary to be known for all agents, and, followers maintain desired time-variant relationships related to the reference input according to maintain time-variant relationships between adjacency agents. Obviously, in the time-variant consensus tracking problem discussed in this note, the time-variant consensus problem and time-variant tracking problem are two independent tasks for agents to be achieved simultaneously.

In recent years, multi-agent system formation problems[8–10] become hot-spots with various achievements such as one-to-one tracking strategies[11], multi-robot synchronization strategies[12], and consensus based strategies[13, 14] etc. In engineering applications of multi-agent coordinations, relative position relationships between agents are general time-variant. On time-varying formation problems, Ref [15–18] proposed consensus-based control strategies for a type of time-varying formations of multi-agent systems, however, the application area of the proposed methods are limited in a special case, where motion of agents are necessary to be described as a fixed formation with respect to a moving coordinate system. Researches on general time-variant formation problems of multi-agent system is few. To solve the general time-variant formation problem, a time-variant consensus tracking control strategy for planar multi-agent systems with non-holonomic constraints is presented in this note. The proposed control strategy is to solve the general time-varying formation and time-varying tracking control problems as long as the desired formation and reference input are both smooth.

In multi-agent system control problems, information exchange between agents via network is necessary. Hence, the networked delay is unavoidable. The observer-based networked predictive control strategy is widely used to compensate the inter-agent communication delay[19–21]. However, in observer-based approaches, the state estimation of a specified agent depends on the agent's control input estimation, and the control input estimation of the specified agent iteratively depends on state estimations of the agent's neighbors, thereby, observers for delay compensation are necessary to be implemented iteratively and repetitively. As thus, the computing efficiency of the multi-agent system is sacrificed for delay compensation. Besides the observer-based compensation strategies, various research results have been achieved on solving the networked delay of multi-agent systems based on specific assumptions. The delay is assumed to be less than one sampling period of controllers in Ref [22]; the derivative of delay is assumed to be bounded in Ref [23]; Ref [24] analyzes the consensus of multi-agent based on Markov chain; and Ref [25] assumes that delay is unknown but constant. Different from mentioned approaches, in this note, an active predictive control strategy is presented to resist the networked delay, where the networked delay is only assumed to be bounded. Obviously, as long as the network is available, there exists a upper bound of the interval between two instants when agents receive valid information from a same adjacency agent. Moreover, in this note, the proposed predictive control strategy is verified via experiments, where the inter-agent communication channels are implemented based on the worldwide networked environments via Aliyun cloud techniques.

The main motivation of this note is to present a solution for general formation problems of planar multi-agent systems with non-holonomic constraints, which is easy to be implemented in engineering application, and suitable for general motion coordination problems of planar multi-agent systems with non-holonomic constraints, so that, with our proposed strategy, complex formation problems can be solved according to design the expected formation (the $\rho_{ij}(t)$ presented in main results) via proven techniques[26, 27] and implement the time-variant formation via our proposed strategy.

As summary, the main contributions of this paper are as follows: (1) A time-variant consensus tracking control strategy for planar non-holonomic multi-agent systems with non-holonomic constraints is presented, under which, the leader is able to track an general smooth time-variant reference input, and followers are able to maintain general smooth time-variant formation simultaneously. (2) An active predictive control strategy is presented for multi-agent system to resist bounded networked delay. Compared with the observer-formed compensation mechanism, the efficiency of the multi-agent system is improved, because it is not necessary to implement observers iteratively and repetitively. Contrast with other strategies in literatures, no special features are imposed to the networked time delay. Moreover, different from most literatures, where research results are verified by numerical simulations, the proposed predictive control strategy is verified by experiments with worldwide networked environments.

2 Planar Non-holonomic Multi-agent System Representation

A planar non-holonomic multi-agent systems is a system composed by multiple planar agents with non-holonomic constraints. Consider a body-fixed coordinate system of a single agent as shown in Fig.1, where rotation center of an agent is regarded as the origin O_r, the X-axis is built along the forward linear velocity, the direction of Z axis is selected as same as the inertial frame, the Y-axis completes the right-hand coordinates. Select a particular point P_i, whose coordinate with respect to the body-fixed coordinate system is $(l, 0)$, $l \neq 0$, denote the coordinate of P_i with respect to the inertial coordinate system as the location of Agent i with respect to the inertial coordinate system, and the angle of the agent's body-fixed coordinate system related to the inertial frame as the orientation of Agent i, then the continuous-time model of the $i-th$

agent of the multi-agent system is expressed as

$$\mathbf{\dot{x}}_i(t) = \begin{bmatrix} \dot{x}_i(t) \\ \dot{y}_i(t) \\ \dot{\varphi}_i(t) \end{bmatrix} = \begin{bmatrix} cos\varphi_i(t) & -l\sin\varphi_i(t) \\ \sin\varphi_i(t) & l\cos\varphi_i(t) \\ 0 & 1 \end{bmatrix} \mathbf{u}_i(t) \quad , i = 0, \dots, n \tag{1}$$
$$\mathbf{y}_i(t) = [x_i(t)\ y_i(t)]^T$$

where $(x_i(t), y_i(t))^T$ is the coordinate of P_i with respect to the inertial frame that represents the position of Agent i, $\varphi_i(t)$ represents agent's orientation, $\mathbf{u}_i(t) = [v_i(t)\ \ \omega_i(t)]^T$ is the control input of Agent i, $v_i(t)$ is the linear velocity and $\omega_i(t)$ is the angular velocity. For convenience, denote

$$\mathcal{R}_i(t) = \begin{bmatrix} \cos\varphi_i(t) & -l\sin\varphi_i(t) \\ \sin\varphi_i(t) & l\cos\varphi_i(t) \end{bmatrix} \tag{2}$$

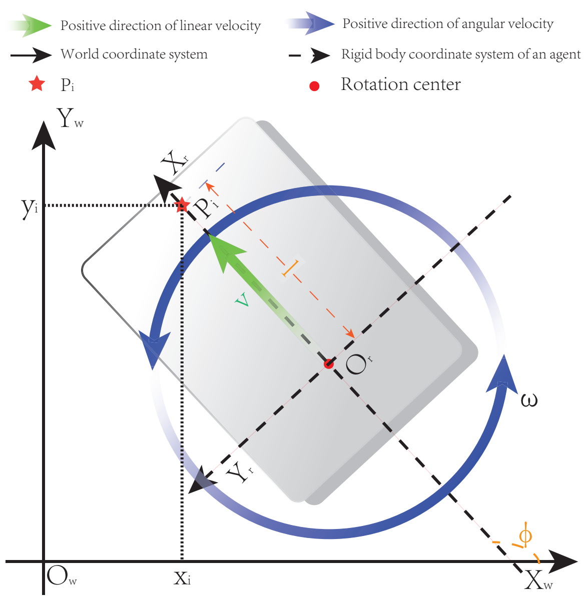

Figure 1: Diagram of the particular point P_i and agent's body-fixed coordinate system

Connect control inputs of agents to zero-order holders i.e. maintain the control input of each agent constants between sampling instants, the continuous-time model (1) is able to be discretized exactly. We consider an engineering background that agents are able to work with same sample period but the sample moments are hardly unified. Fig 2 shows a diagram about offsets on sample moments of the multi-agent systems,where $\Delta\varepsilon_{ij}$ is defined as

$$\Delta\varepsilon_{ij} = \begin{cases} \varepsilon_j - \varepsilon_i - T & \varepsilon_j > \varepsilon_i \\ \varepsilon_j - \varepsilon_i & otherwise \end{cases} \tag{3}$$

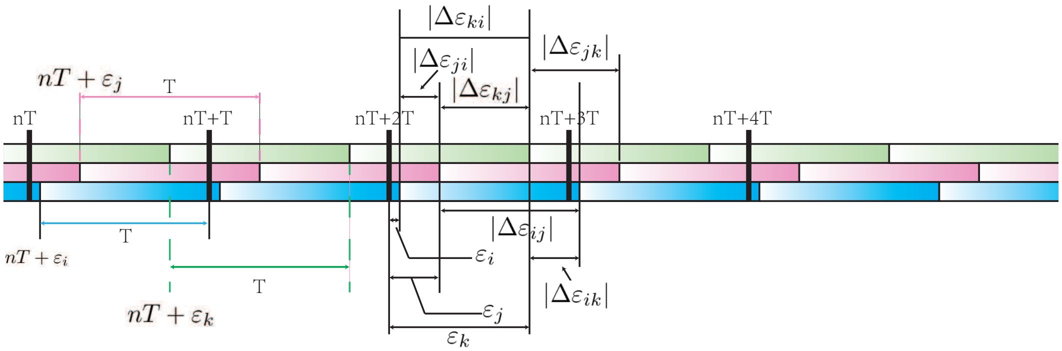

Figure 2: Diagram of offset on sample moments of different agents

According to Fig.2, the sample moments of the $i-th$ agent is expressed as $kT+\varepsilon_i$, where $k\in\mathbb{Z}^+$ and ε_i is the offset of the sample system of $i-th$ agent. Denote $s_i^k=kT+\varepsilon_i$, the discrete-time model of the multi-agent system composed by $n+1$ planar non-holonomic agents are expressed as

$$\begin{array}{l}\mathbf{x}_i(s_i^{(k+1)})=\mathbf{x}_i(s_i^k)+\mathcal{B}_i(s_i^k)\mathbf{u}_i(s_i^k)\\ \mathbf{y}_i(s_i^k)=\left[x_i(s_i^k)\ y_i(s_i^k)\right]\end{array},i=0,\ldots,n \tag{4}$$

where

$$\mathcal{B}_i(s_i^k)=\begin{bmatrix}\beta_i(s_i^k)\Psi_i(s_i^k)\\ 0\quad T\end{bmatrix}_{3\times2},\qquad \beta_i(s_i^k)=\begin{cases}T & \omega_i(s_i^k)=0\\ 2\frac{\sin\left(\frac{T}{2}\omega_i(s_i^k)\right)}{\omega_i(s_i^k)} & otherwise\end{cases},$$

$$\Psi_i(s_i^k)=\begin{bmatrix}\cos\psi_i(s_i^k) & -l\sin\psi_i(s_i^k)\\ \sin\psi_i(s_i^k) & l\cos\psi_i(s_i^k)\end{bmatrix},\quad \psi_i(s_i^k)=\varphi_i(s_i^k)+\tfrac{T}{2}\omega_i(s_i^k)$$

Note that, according to the Euler exact discretization, (4) is continuous at $\omega_i(s_i^k)=0$.

3 Unidirectional Topology Structure Representation and Agent Index

In this note, an unidirectional topology structure(topology structure is directed, but messages are only transferred in the direction from the root node to leaf-nodes) is adopted to design the time-variant consensus tracking control strategy. A digraph $\mathcal{G}=\{\mathcal{V},\mathcal{E},\mathcal{A}\}$ is adopted to describe the communication topology structure of the multi-agent system, where $\mathcal{V}$ is a finite nonempty set of vertexes, $\mathcal{E}$ is a finite nonempty set of edges, and $\mathcal{A}$ is an adjacency matrix with $a_{ij}>0$ if and only if $(v_j,v_i)\in\mathcal{E}$ and $a_{ij}=0$ otherwise. The topology structure $\mathcal{G}$ to implement the proposed time-variant consensus tracking control strategy is necessary to satisfy following conditions: (1) $\mathcal{G}$ contains a spanning tree with the leader agent as the root node; (2) The leader is indexed as Agent 0, and the followers are indexed incrementally, from 1 to n according to the breadth-first traversal[28] of the spanning tree; (3) $\forall 0\le i<j\le n$, $a_{ij}=0$ i.e. Agent i only receive messages from agents with indexes less than i. (4) $\forall i=1,\ldots,n,\sum_{j=0}^{i-1}a_{ij}=1$.

For easy to understand the unidirectional topology structure, a diagram of the unidirectional topology structure is given as Fig.3. As shown in Fig.3, the unidirectional topology structure is able to be roughly regarded as a tree whose nodes are indexed incrementally according to the breadth-first traversal, plus additional edges from nodes with less index to ones with more index.

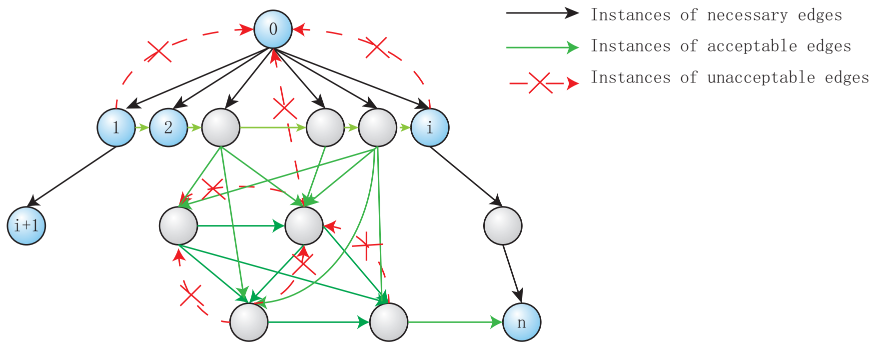

Figure 3: A diagram of the unidirectional topology structure

On the basis of the digraph $\mathcal{G}$, for Agent i, define d_i as the maximum number of nodes on each path from Agent i to reachable leaf-nodes (including Agent i and the leaf-node). In $\mathcal{G}$, leaf-nodes represent agents who has no followers i.e. Agent l is called leaf-node as long as $\forall k = 0, \ldots, n, l \neq k, a_{kl} = 0$.

4 Time-variant Consensus Tracking Problem

In the time-variant consensus tracking problem, the leader agent is expected to track a desired smooth reference trajectory and the follower agents are expected to maintain a desired smooth time-variant formation with the leader. A group of time-variant vectors are adopted to describe the desired formation, where $\rho_{ji}(t)$ represents the desired position output of Agent i related to Agent j at time t. Vector $\rho_{ri}(t)$ is adopted to describe the desired position output of Agent i related to the reference input at time t, particularly $\rho_{r0}(t) \triangleq 0$.

Define the consensus tracking error of Agent i as

$$\mathbf{e}_i(t) = \mathbf{y}_i(t) - \mathbf{r}(t) - \rho_{ri}(t), i = 0, \ldots, n \tag{5}$$

where $\mathbf{r}(t)$ is the reference input at time t. The time-variant consensus tracking for the multi-agent system described as (4) is reached as long as the consensus tracking error of each agent converges into a neighborhood of the origin as

$$\lim_{t \to +\infty} \|\mathbf{e}_i(t)\| < \delta, \forall i = 0, \ldots, n \tag{6}$$

where δ is a positive constant representing the ultimate bound of the steady state error.

According to the rules of vector operations, it is obvious

$$\rho_{ji}(t) = -\rho_{ij}(t) = \rho_{0i}(t) - \rho_{0j}(t) = \rho_{ri}(t) - \rho_{rj}(t) \tag{7}$$

To simplify the representation of the application background, we make some assumptions first: (1) The maximum delay of message from adjacency agents for each agent caused by networked communication delay and packet loss is bounded by MT, where $M \in \mathbb{Z}^+$, and T is the sampling period of controllers of agents; (2) Time of the multi-agent system is synchronized, and packets of agents are transferred with time stamps; (3) The desired time-variant formation $\rho_{ij}(t)$,$i, j = 0, \ldots, n, i \neq j$, is known and smooth; (4) For Agent 0, at time t, the desired trajectory from time t to $t + d_0MT$ is known, and the reference input is smooth.

5 Control System Designing

In this section, we are going to define some denotations first, then represent the design of control laws, and finally give the active predictive compensation scheme.

Define

$$\begin{aligned}
\widehat{\mathcal{R}}_i(t|t^*) &= \begin{bmatrix} \cos\widehat{\varphi}_i(t|t^*) & -l\sin\widehat{\varphi}_i(t|t^*) \\ \sin\widehat{\varphi}_i(t|t^*) & l\cos\widehat{\varphi}_i(t|t^*) \end{bmatrix}, \\
\widehat{\psi}_i(s_i^{(k+m)}|s_i^k) &= \widehat{\varphi}_i(s_i^{(k+m)}|s_i^k) + \tfrac{T}{2}\widehat{\omega}_i(s_i^{(k+m)}|s_i^k) \\
\widehat{\beta}_i(s_i^{(k+m)}|s_i^k) &= \begin{cases} T & \omega_i(s_i^{(k+m)}|s_i^k) = 0 \\ 2\frac{\sin\left(\frac{T}{2}\widehat{\omega}_i(s_i^{(k+m)}|s_i^k)\right)}{\widehat{\omega}_i(s_i^{(k+m)}|s_i^k)} & otherwise \end{cases}, \\
\widehat{\Psi}_i(s_i^{(k+m)}|s_i^k) &= \begin{bmatrix} \cos\widehat{\psi}_i(s_i^{(k+m)}|s_i^k) & -l\sin\widehat{\psi}_i(s_i^{(k+m)}|s_i^k) \\ \sin\widehat{\psi}_i(s_i^{(k+m)}|s_i^k) & l\cos\widehat{\psi}_i(s_i^{(k+m)}|s_i^k) \end{bmatrix}, \\
\widehat{\mathcal{B}}_i(s_i^{(k+m)}|s_i^k) &= \begin{bmatrix} \widehat{\beta}_i(s_i^{(k+m)}|s_i^k)\widehat{\Psi}_i(s_i^{(k+m)}|s_i^k) \\ 0 \quad T \end{bmatrix},
\end{aligned}$$

and

$$\mathbf{K}_i = \begin{bmatrix} k_{ix} & 0 \\ 0 & k_{iy} \end{bmatrix}, i = 0, \ldots, n \tag{8}$$

where $k_{ix}, k_{iy} \in (0, 1)$ are tunable positive constant parameters.

Define

$$\widetilde{\Psi}_i(s_i^k) = \begin{bmatrix} \cos\widetilde{\psi}_i(s_i^k) & -l\sin\widetilde{\psi}_i(s_i^k) \\ \sin\widetilde{\psi}_i(s_i^k) & l\cos\widetilde{\psi}_i(s_i^k) \end{bmatrix} \tag{9}$$

where

$$\widetilde{\psi}_i(s_i^k) = \varphi_i(s_i^k) + \frac{T}{2}\omega_i(s_i^{(k-1)}) \tag{10}$$

and $\mathcal{F}(\cdot) : \mathbb{R}^2 \to \mathbb{R}^2$ as

$$\mathcal{F}([\mu_1 \ \mu_2]^T) = \begin{cases} \left[\frac{1}{T}\mu_1 \ 0\right]^T & \mu_2 = 0 \\ \frac{1}{T}\arcsin\mu_2 \begin{bmatrix}\frac{\mu_1}{\mu_2} & 1\end{bmatrix}^T & otherwise \end{cases} \tag{11}$$

Note that $\mathcal{F}(\cdot)$ is invertible

$$\mathcal{F}^{-1}([v_i(t)\ \omega_i(t)]^T) = \begin{cases} T\,[v_i(t)\ 0] & \omega_i(t)=0 \\ 2\frac{\sin\left(\frac{T}{2}\omega_i(t)\right)}{\omega_i(t)}\,[v_i(t)\ \omega_i(t)]^T & otherwise \end{cases} \tag{12}$$

To guarantee that for each agent, the initial state of adjacency agents are known under the networked delay, a start moment $t_s = d_0MT$ is set up, before which all agents maintain the initial states with zero control inputs. The tracking control law of Agent 0 is designed as

$$\begin{aligned} \mathbf{u}_0(s_0^k) =& k_l\left(\mathbf{x}_0(s_0^k), \mathbf{r}(s_0^k), \mathbf{r}(s_0^{(k+1)})\right) \qquad (13)\\ =& \begin{cases} 0 & s_0^k < t_s \\ \mathcal{F}\left(\widetilde{\Psi}_i^{-1}(s_i^k)\left(\left(\mathbf{K}_0 - \mathbf{I}\right)\mathbf{y}_0(t) + \mathbf{r}(s_0^{(k+1)}) - \mathbf{K}_0\mathbf{r}(s_0^k)\right)\right) & s_0^k \geq t_s \end{cases} \end{aligned}$$

where $\mathbf{I}$ is the unit matrix. Note that, since the discrete-time model of the multi-agents system is obtained via control input zero holders, for each Agent i, as long as predictions from Agent j is received, the state predictions of Agent j at sampling instants of Agent i are able to be obtained as

$$\begin{aligned} &\widehat{\mathbf{x}}_j(s_i^k|s_i^k - \tau_{ij}(s_i^k)) \qquad (14)\\ =&\widehat{\mathbf{x}}_j(s_i^k + \Delta\varepsilon_{ij}|s_i^k - \tau_{ij}(s_i^k)) + \int_{s_i^k+\Delta\varepsilon_{ij}}^{s_i^k} \widehat{\mathcal{R}}_j(\lambda|s_i^k - \tau_{ij}(s_i^k))d\lambda\widehat{\mathbf{u}}_j(s_i^k + \Delta\varepsilon_{ij}|s_i^k - \tau_{ij}(s_i^k)) \end{aligned}$$

and the control input prediction of Agent j in the duration $\left[s_i^{(k+m)}, s_i^{(k+m+1)}\right)$ is able to be represented as

$$\begin{aligned} &\widehat{\mathbf{u}}_j(\lambda|s_i^k - \tau_{ij}(s_i^k)) \qquad (15)\\ =&\begin{cases} \widehat{\mathbf{u}}_j(s_i^{(k+m)} + \Delta\varepsilon_{ij}|s_i^k - \tau_{ij}(s_i^k)) & \lambda \in \left[s_i^{(k+m)}, s_i^{(k+m)} + T + \Delta\varepsilon_{ij}\right) \\ \widehat{\mathbf{u}}_j(s_i^{(k+m+1)} + \Delta\varepsilon_{ij}|s_i^k - \tau_{ij}(s_i^k)) & \lambda \in \left[s_i^{(k+m)} + T + \Delta\varepsilon_{ij}, s_i^{(k+m)} + T\right) \end{cases} \end{aligned}$$

Define

$$\widehat{\mathbf{X}}_i(s_i^k) = \left\{\widehat{\mathbf{x}}_j(s_i^k|s_i^k - \tau_{ij}(s_i^k))|a_{ij} > 0, j = 0, \ldots, i-1\right\} \tag{16}$$

$$\widehat{\mathbf{U}}_i(s_i^k) = \left\{\widehat{\mathbf{u}}_j(\lambda|s_i^k - \tau_{ij}(s_i^k))|\lambda \in \left[s_i^k, s_i^{(k+1)}\right), a_{ij} > 0, j = 0, \ldots, i-1\right\} \tag{17}$$

The consensus control law of Agent i, $i = 1, \ldots, n$, is designed as

$$\mathbf{u}_i(s_i^k) = k_f\left(\mathbf{x}_i(s_i^k), \widehat{\mathbf{X}}_i(s_i^k), \widehat{\mathbf{U}}_i(s_i^k)\right) \tag{18}$$

$$= \begin{cases} 0 & s_i^k < t_s \\ \mathcal{F}\left(\widetilde{\Psi}_i^{-1}(s_i^k)\left(\sum_{j=0}^{i-1} a_{ij}\widehat{\Lambda}_{ij}(s_i^k)\right)\right) & s_i^k \geq t_s \end{cases} \tag{19}$$

where

$$
\begin{aligned}
&\widehat{\Lambda}_{ij}(s_i^k) = (\mathbf{K}_i - \mathbf{I})\left(\mathbf{y}_i(s_i^k) - \widehat{\mathbf{y}}_j(s_i^k|s_i^k - \tau_{ij}(s_i^k)) - \rho_{ji}(s_i^k)\right) + \widehat{\mathcal{Q}}_j(s_i^k|s_i^k - \tau_{ij}(s_i^k)) + \Delta\rho_{ji}(s_i^k) \\
&\widehat{\mathcal{Q}}_{ij}(s_i^k|s_i^k - \tau_{ij}(s_i^k)) = \int_{s_i^k}^{s_i^{(k+1)}} \widehat{\mathcal{R}}_j(\lambda|s_i^k - \tau_{ij}(s_i^k))\widehat{\mathbf{u}}_j(\lambda|s_i^k - \tau_{ij}(s_i^k))d\lambda \\
&\Delta\rho_{ji}(s_i^k) = \rho_{ji}(s_i^{k+1}) - \rho_{ji}(s_i^k)
\end{aligned}
$$

and $\tau_{ij}(t)$ is the delay of information of Agent j for Agent i at time t. Since $\widehat{\mathcal{R}}_j(\lambda)$ is piecewise constant at $\left[s_i^k, s_i^{(1)}\right)$, $\widehat{\mathcal{Q}}_{ij}(s_i^k|s_i^k - \tau_{ij}(s_i^k))$ is easy to calculate.

The one step forward state prediction of the $i-th$ agent is given as

$$
\widehat{\mathbf{x}}_i(s_i^{(k+1)}|s_i^k) = \mathbf{x}_i(s_i^k) + \mathcal{B}_i(s_i^k)\mathbf{u}_i(s_i^k) \tag{20}
$$

Based on the one step forward state prediction, subsequent predictions at sampling instants are given iteratively:

$$
\widehat{\mathbf{u}}_0(s_0^{k+m}|s_0^k) = k_l\left(\widehat{\mathbf{x}}_0(s_0^{k+m}|s_0^k), \mathbf{r}(s_0^{k+m}), \mathbf{r}(s_0^{k+m+1})\right) \tag{21}
$$

$$
\widehat{\mathbf{u}}_j(s_j^{(k+m)}|s_j^k) = k_f\left(\mathbf{x}_j(s_j^{(k+m)}|s_j^k), \widehat{\mathbf{X}}_j(s_j^{(k+m)}), \widehat{\mathbf{U}}_j(s_j^{(k+m)})\right) \tag{22}
$$

$$
\widehat{\mathbf{x}}_i(s_i^{k+m+1}|s_i^k) = \widehat{\mathbf{x}}_i(s_i^{k+m}|s_i^k) + \widehat{\mathcal{B}}_i(s_i^{k+m}|s_i^k)\widehat{\mathbf{u}}_i(s_i^{k+m}|s_i^k), \tag{23}
$$

where $j = 1, \ldots, n$, $i = 0, \ldots, n$, $m = 1, \ldots, (d_i + 1)M$. Based on the given predictions, Agent i transmits the packet described as (24) to its reachable neighbors.

$$
\mathcal{P}_i(s_i^k) = \begin{bmatrix} \mathbf{x}_i(s_i^k) & \widehat{\mathbf{x}}_i(s_i^{(k+1)}|s_i^k) & \ldots & \widehat{\mathbf{x}}_i(s_i^k + (d_i+1)MT|s_i^k) \\ \mathbf{u}_i(s_i^k) & \widehat{\mathbf{u}}_i(s_i^{(k+1)}|s_i^k) & \ldots & \widehat{\mathbf{u}}_i(s_i^k + (d_i+1)MT|s_i^k) \end{bmatrix} \tag{24}
$$

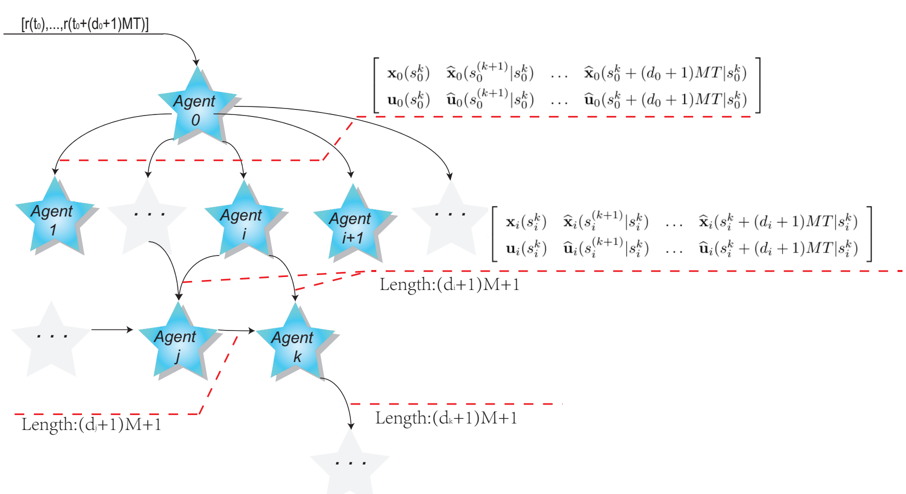

Figure 4: Diagram of the unidirectional topology structure and the active prective mechanism

Fig.4 illustrates the packet transferring procedure of the active predictive compensation mechanism. The lengths of packets are various. As long as Agent i is a non-leaf node (a node with followers), it generates $(d_i+1)M$ pairs of its state and control input predictions and transmits the predictions to its reachable neighbors. The packet length of each agent in the proposed prediction scheme is able to guarantee that, the number of available predictions for receivers are enough to generate their own predictions iteratively after networked transferring.

6 Stability Analysis

Theorem 6.1 *Consider a planar multi-agent system with non-holonomic constraints described as (4) with $i=0,\ldots,n$, under the predictive consensus tracking control strategy described as (13), (18), (20), (21), (22), (23), and (24), for arbitrary Agent i, $i=0,\ldots,n$, the consensus tracking error $\mathbf{e}_i(t)$ converges into a neighborhood of the origin exponentially i.e.*

$$\lim_{t\to+\infty}\|\mathbf{e}_i(t)\|<\delta \tag{25}$$

as long as

$$\|\mathbf{K}_i\|+\max(\|\Gamma_i(t)\|)\,\|\mathbf{K}_i-\mathbf{I}\|<1 \tag{26}$$

where

$$\Gamma_i(s_i^k)=\mathbf{I}-\Psi_i(s_i^k)\widetilde{\Psi}_i^{-1}(s_i^k)=\begin{bmatrix}\sin^2(\frac{T}{4}(\omega_i(s_i^k)-\omega_i(s_i^{(k-1)})) & \sin(\frac{T}{2}(\omega_i(s_i^k)-\omega_i(s_i^{(k-1)})) \\ -\sin(\frac{T}{2}(\omega_i(s_i^k)-\omega_i(s_i^{(k-1)})) & \sin^2(\frac{T}{4}(\omega_i(s_i^k)-\omega_i(s_i^{(k-1)}))\end{bmatrix}$$

Proof Note that the output evolution of the $i-th$ agent is expressed as

$$\begin{aligned}\mathbf{y}_i(s_i^{(k+1)})=&\mathbf{y}_i(s_i^k)+\beta_i(s_i^k)\Psi_i(s_i^k)\mathbf{u}_i(s_i^k)\\ =&\mathbf{y}_i(s_i^k)+\Psi_i(s_i^k)\mathcal{F}^{-1}\left(\mathbf{u}_i(s_i^k)\right)\end{aligned} \tag{27}$$

Consider the Agent 0, substituting (13),(27) into (5), for $k\geq(d_0+1)M$, the error state dynamics is obtained:

$$\begin{aligned}\mathbf{e}_0(s_0^{(k+1)})=&\mathbf{y}_0(s_0^k)+\mathcal{B}_0(s_0^k)\mathbf{u}_0(s_0^k)-\mathbf{r}(s_0^{(k+1)})\\ =&\mathbf{y}_0(s_0^k)+\mathcal{B}_0(s_0^k)\mathcal{F}\left(\widetilde{\Psi}_0^{-1}(s_0^k)\left(\left(\mathbf{K}_0-\mathbf{I}\right)\mathbf{y}_0(s_0^k)+\mathbf{r}(s_0^{(k+1)})-\mathbf{K}_0\mathbf{r}(s_0^k)\right)\right)-\mathbf{r}(s_0^{(k+1)})\\ =&\mathbf{y}_0(s_0^k)+\Psi_0(s_0^k)\mathcal{F}^{-1}\left(\mathcal{F}\left(\widetilde{\Psi}_0^{-1}(s_0^k)\left(\left(\mathbf{K}_0-\mathbf{I}\right)\mathbf{y}_0(s_0^k)+\mathbf{r}(s_0^{(k+1)})-\mathbf{K}_0\mathbf{r}(s_0^k)\right)\right)\right)\\ &-\mathbf{r}(s_0^{(k+1)})\\ =&\mathbf{K}_0\mathbf{e}_0(s_0^k)-\Gamma_0(s_0^k)\left(\left(\mathbf{K}_0-\mathbf{I}\right)\mathbf{y}_0(s_0^k)+\mathbf{r}(s_0^{(k+1)})-\mathbf{K}_0\mathbf{r}(s_0^k)\right)\\ =&\mathbf{K}_0\mathbf{e}_0(s_0^k)-\Gamma_0(s_0^k)\left(\mathbf{K}-\mathbf{I}\right)\mathbf{e}_0(s_0^k)-\Gamma_0(s_0^k)\Delta\mathbf{r}(s_0^k)\end{aligned} \tag{28}$$

where $\Delta\mathbf{r}(s_0^k)=\mathbf{r}(s_0^{(k+1)})-\mathbf{r}(s_0^k)$

According to the definition of $\Gamma_i(s_i^k)$, it is obtained that $\left\|\Gamma_i(s_i^k)\right\|$ is bounded as

$$\left\|\Gamma_i(s_i^k)\right\| < c_1, \forall i = 0, \dots, n, k \in \mathbb{Z}^+ \tag{29}$$

Since $\mathbf{r}(t)$ is smooth, it is able to guarantee that $\|\Delta\mathbf{r}(t)\|$ is bounded as

$$\|\Delta\mathbf{r}(t)\| < c_2 \tag{30}$$

Taking norm on (28), the following is obtained:

$$\left\|\mathbf{e}_0(s_0^{(k+1)})\right\| \le (\|\mathbf{K}\| + c_1 \|\mathbf{K}_0 - \mathbf{I}\|) \left\|\mathbf{e}_0(s_0^k)\right\| + c_1 c_2 \tag{31}$$

According to the condition described by (26), the following is obtained:

$$\lim_{k\to+\infty} \left\|\mathbf{e}_0(s_0^k)\right\| \le \frac{c_1 c_2}{1 - (\|\mathbf{K}\| + c_1 \|\mathbf{K}_0 - \mathbf{I}\|)} \tag{32}$$

Moreover,

$$\lim_{t\to+\infty} \|\mathbf{e}_0(t)\| < \delta \tag{33}$$

where δ is the positive constant.

Without uncertainty, compare (20),(21),(23) with (4) and (13), and let $i = 0$, the prediction sequence is obtained:

$$\begin{aligned}
\widehat{\mathbf{x}}_0(s_0^{(k+1)}|s_0^k) =& \mathbf{x}_0(s_0^k) + \mathcal{B}_0(s_0^k)\mathbf{u}_0(s_0^k) = \mathbf{x}_0(s_0^{(k+1)}) \\
\widehat{\mathbf{x}}_0(s_0^{(k+m+1)}|s_0^k) =& \widehat{\mathbf{x}}_0(s_0^{(k+m)}|s_0^k) + \widehat{\mathcal{B}}_0(s_0^{(k+m)}|s_0^k)\widehat{\mathbf{u}}_0(s_0^{(k+m)}|s_0^k) \\
=& \mathbf{x}_0(s_0^{(k+m)}) + \mathcal{B}_0(s_0^{(k+m)})\mathbf{u}_0(s_0^{(k+m)}) \\
=& \mathbf{x}_0(s_0^{(k+m+1)}) \\
\widehat{\mathbf{u}}_0(s_0^{(k+m)}|s_0^k) =& k_l\left(\widehat{\mathbf{x}}_0(s_0^{(k+m)}|s_0^k), \mathbf{r}(s_0^{(k+m)}), \mathbf{r}(s_0^{(n+k+1)})\right) \\
=& k_l\left(\mathbf{x}_0(s_0^{(k+m)}), \mathbf{r}(s_0^{(k+m)}), \mathbf{r}(s_0^{(n+k+1)})\right) \\
=& \mathbf{u}_0(s_0^{(k+m)})
\end{aligned}$$

where $k \in \mathbb{Z}^+, m = 1, \dots, (d_0+1)M$.

It shows that under the proposed predictive control strategy, $\|\mathbf{e}_0(t)\|$ converges into a neighborhood of the origin exponentially, and, without uncertainty, the predicted states and control inputs of Agent 0 are equivalent to the actual ones.

Next, the mathematical induction is adopted to analyze stability performance of followers. For each Agent i, $i = 1, \dots, n$, assume that consensus tracking errors of agents with indexes less than i converge into a neighborhood of the origin as

$$\lim_{t\to+\infty} \|\mathbf{e}_p(t)\| < \delta, \forall p = 0, \dots, i-1 \tag{34}$$

and for arbitrary Agent p, $p = 0, \dots, i-1$, the predicted states and control inputs are equivalent to the actual ones as

$$\widehat{\mathbf{x}}_p\left(s_p^{(k+m)}|s_p^k\right) = \mathbf{x}_p\left(s_p^{(k+m)}\right), \forall\, p = 0, \dots, i-1, \forall m = 1, \dots, (d_p+1)M \tag{35}$$

$$\widehat{\mathbf{u}}_p\left(s_p^{(k+m)}|s_p^k\right) = \mathbf{u}_p\left(s_p^{(k+m)}\right), \forall\, p = 0, \dots, i-1, \forall m = 1, \dots, (d_p+1)M \tag{36}$$

According to the Euler discretization, for each sample moment s_i^k of Agent i, the following is obtained:

$$\begin{aligned}
&\widehat{\mathbf{y}}_p(s_i^{(k+m)}|s_i^k - \tau_{ij}(s_i^k)) \\
=&\widehat{\mathbf{y}}_p(s_i^{(k+m)} + \Delta\varepsilon_{ij}|s_i^k - \tau_{ij}(s_i^k)) + \int_{s_i^{(k+m)}+\Delta\varepsilon_{ij}}^{s_i^{(k+m)}} \widehat{\mathcal{R}}_p(\lambda|s_i^k - \tau_{ij}(s_i^k))d\lambda\widehat{\mathbf{u}}_p(s_i^{(k+m)} + \Delta\varepsilon_{ij}|s_i^k - \tau_{ij}(s_i^k)) \\
=&\mathbf{y}_p(s_i^{(k+m)} + \Delta\varepsilon_{ij}) + \int_{s_i^{(k+m)}+\Delta\varepsilon_{ij}}^{s_i^{(k+m)}} \mathcal{R}_p(\lambda)d\lambda\mathbf{u}_p(s_i^{(k+m)} + \Delta\varepsilon_{ij}) \\
=&\mathbf{y}_p(s_i^{(k+m)})
\end{aligned} \tag{37}$$

$$\begin{aligned}
&\widehat{\mathbf{y}}_p(s_i^{(k+m)}|s_i^k - \tau_{ij}(s_i^k)) + \widehat{\mathcal{Q}}_p(s_i^{(k+m)}|s_i^k - \tau_{ij}(s_i^k)) \\
=&\widehat{\mathbf{y}}_p(s_i^{(k+m)}|s_i^k - \tau_{ij}(s_i^k)) + \int_{s_i^{(k+m)}}^{s_i^{(k+1)}} \widehat{\mathcal{R}}_p(\lambda|s_i^k - \tau_{ij}(s_i^k))\widehat{\mathbf{u}}_p(\lambda|s_i^k - \tau_{ij}(s_i^k))d\lambda \\
=&\mathbf{y}_p(s_i^{(k+m)}) + \int_{s_i^{(k+m)}}^{s_i^{(k+m+1)}} \mathcal{R}_p(\lambda)\mathbf{u}_p(\lambda)d\lambda \\
=&\mathbf{y}_p(s_i^{(k+m+1)})
\end{aligned} \tag{38}$$

$$\forall m = 0, \dots, (d_i+1)M$$

Then, for $s_i^k \geq t_s$, it is given:

$$\begin{aligned}
\mathbf{e}_i(s_i^{(k+1)}) =&\mathbf{y}_i(s_i^k) + \mathcal{B}_i(s_i^k)\mathbf{u}_i(s_i^k) - \rho_{ri}(s_i^{(k+1)}) \\
=&\mathbf{y}_i(s_i^k) + \Psi_i(s_i^k)\mathcal{F}^{-1}\left(\mathcal{F}\left(\widetilde{\Psi}_i^{-1}(s_i^k)\sum_{j=0}^{i-1} a_{ij}\widehat{\Lambda}_{ij}(s_i^k)\right)\right) - \rho_{ri}(s_i^{(k+1)}) \\
=&\sum_{j=0}^{i-1} a_{ij}\Bigg(\mathbf{K}_i\left(\mathbf{y}_i(s_i^k) - \mathbf{y}_j(s_i^k) - \rho_{ji}(s_i^k)\right) + \mathbf{y}_j(s_i^{(k+1)}) + \rho_{ji}(s_i^{(k+1)}) \\
&- \rho_{ri}(s_i^{(k+1)}) - \Gamma_i(s_i^k)\widehat{\Lambda}_{ij}(s_i^k)\Bigg)
\end{aligned} \tag{39}$$

Note that

$$\rho_{ji}(t) = \rho_{ri}(t) - \rho_{rj}(t) \tag{40}$$

therefore, without uncertainty,

$$\begin{aligned}\mathbf{e}_i(s_i^{(k+1)}) =&\mathbf{K}_i\mathbf{e}_i(s_i^k) + \sum_{j=0}^{i-1} a_{ij}\left(\mathbf{e}_j(s_i^{(k+1)}) - \mathbf{K}_i\mathbf{e}_j(s_i^k) - \Gamma_i(s_i^k)\Lambda_{ij}(s_i^k)\right)\\ =&\mathbf{K}_i\mathbf{e}_i(s_i^k) - \Gamma_i(s_i^k)\left(\mathbf{K}-\mathbf{I}\right)\mathbf{e}_i(s_i^k) + \sum_{j=0}^{i-1} a_{ij}\left(\mathbf{e}_j(s_i^{(k+1)}) - \mathbf{K}_i\mathbf{e}_j(s_i^k)\right.\\ &\left. - \Gamma_i(s_i^k)\left(\left(\mathbf{I}-\mathbf{K}\right)\mathbf{e}_j(s_i^k) + \int_{s_i^k}^{s_i^{(k+1)}} \mathcal{R}(\lambda)\mathbf{u}_j(\lambda)d\lambda + \Delta\rho_{ji}(s_i^k)\right)\right) \end{aligned} \tag{41}$$

Taking norm on (41), it is given:

$$\begin{aligned}\left\|\mathbf{e}_i(s_i^{(k+1)})\right\| \leq& \left(\|\mathbf{K}_i\| + c_1\|\mathbf{K}_i-\mathbf{I}\|\right)\left\|\mathbf{e}_i(s_i^k)\right\| + \left\|\mathbf{e}_q(s_i^{(k+1)}) - \mathbf{K}_i\mathbf{e}_q(s_i^k)\right\|\\ &+ c_1\left\|\left(\mathbf{I}-\mathbf{K}_i\right)\mathbf{e}_j(s_i^k) + \int_{s_i^k}^{s_i^{(k+1)}} \mathcal{R}_q(\lambda)\mathbf{u}_q(\lambda)d\lambda + \Delta\rho_{mi}(s_i^k)\right\| \end{aligned} \tag{42}$$

where $0 \leq q < i$ and $a_{iq} > 0$. It can be given by (34) that

$$\left\|\mathbf{e}_q(s_i^{(k+1)}) - \mathbf{K}_i\mathbf{e}_q(s_i^k)\right\| < c_3 \tag{43}$$

$$\left\|\left(\mathbf{I}-\mathbf{K}_i\right)\mathbf{e}_j(s_i^k)\right\| < c_4 \tag{44}$$

$$\left\|\int_{s_i^k}^{s_i^{(k+1)}} \mathcal{R}_q(\lambda)\mathbf{u}_q(\lambda)d\lambda\right\| = \left\|\mathbf{y}_q(s_i^{(k+1)}) - \mathbf{y}_q(s_i^k)\right\| < c_5 \tag{45}$$

Since $\rho_{ji}(t)$ is smooth, it is clear that

$$\left\|\Delta\rho_{ji}(s_i^k)\right\| < c_6 \tag{46}$$

Denote $c_7 = c_3 + c_1(c_4 + c_5 + c_6)$, (42) can be rewritten as

$$\left\|\mathbf{e}_i(s_i^{(k+1)})\right\| \leq \left(\|\mathbf{K}_i\| + c_1\|\mathbf{K}_i-\mathbf{I}\|\right)\left\|\mathbf{e}_i(s_i^k)\right\| + c_7 \tag{47}$$

Then, the ultimate bound of $\|\mathbf{e}_i(t)\|$ can be obtained as

$$\lim_{k\to+\infty}\left\|\mathbf{e}_i\left(s_i^k\right)\right\| \leq \frac{c_7}{1-\left(\|\mathbf{K}_i\| + c_1\|\mathbf{K}_i-\mathbf{I}\|\right)} \tag{48}$$

Moreover,

$$\lim_{t\to+\infty}\|\mathbf{e}_i(t)\| < \delta \tag{49}$$

Without uncertainty, comparing (20),(22) ,(23)with (4) and (18), and combing (35) and

(36), the prediction equivalency can be obtain as

$$
\begin{aligned}
\widehat{\mathbf{x}}_i(s_i^{(k+1)}|s_i^k) =&\mathbf{x}_i(s_i^k) + \mathcal{B}_i(s_i^k)\mathbf{u}_i(s_i^k) = \mathbf{x}_i(s_i^{(k+1)}) \\
\widehat{\mathbf{x}}_i(s_i^{(k+m+1)}|s_i^k) =&\widehat{\mathbf{x}}_i(s_i^{(k+m)}|s_i^k) + \widehat{\mathcal{B}}_i(s_i^{(k+m)}|s_i^k)\widehat{\mathbf{u}}_i(s_i^{(k+m)}|s_i^k) \\
=&\mathbf{x}_i(s_i^{(k+m)}) + \mathcal{B}_i(s_i^{(k+m)})\mathbf{u}_i(s_i^{(k+m)}) \\
=&\mathbf{x}_i(s_i^{(k+m+1)}) \\
\widehat{\mathbf{u}}_i(s_i^{(k+m)}) =&k_f\left(\widehat{\mathbf{x}}_i(s_i^{(k+m)}|s_i^k), \widehat{\mathbf{X}}_i(s_i^{(k+m)}), \widehat{\mathbf{U}}_i(s_i^{(k+m)})\right) \\
=&k_f\left(\mathbf{x}_i(s_i^{(k+m)}), \mathbf{X}_i(s_i^{(k+m)}), \mathbf{U}_i(s_i^{(k+m)})\right) \\
=&\mathbf{u}_i(s_i^{(k+m)}) \\
&\forall m = 0, \ldots, (d_i+1)M
\end{aligned} \tag{50}
$$

where

$$
\mathbf{X}_i(s_i^{(k+m)}) = \left\{\mathbf{x}_j(s_i^{(k+m)}|a_{ij} > 0, j = 0, \ldots, i-1\right\} \tag{51}
$$

$$
\mathbf{U}_i(s_i^{(k+m)}) = \left\{\mathbf{u}_j(\lambda)|\lambda \in \left[s_i^{(k+m)}, s_i^{(k+m+1)}\right), a_{ij} > 0, j = 0, \ldots, i-1\right\} \tag{52}
$$

As summary, under the proposed predictive control strategy described as (13), (18), (20), (21), (22) and (23), for Agent 0, the consensus tracking error converges into a neighborhood of the origin and, without uncertainty, the predicted states and control inputs are equivalent to the actual ones; Moreover as long as it is assumed that, for all agents with indexes less than i, the tracking errors converge into a neighborhood of the origin and the predicted states and control inputs are equivalent to the actual ones, it is able to obtain that consensus tracking error of Agent i also converges into the neighborhood of the origin and the predicted states and control inputs are equivalent to the actual one as well. Therefore, according to the mathematical induction, it is clear that for arbitrary Agent i, $i = 0, \ldots, n$, under the proposed predictive control strategy, the consensus tracking error $\mathbf{e}_i(t)$ converges into a neighborhood of the origin, and, without uncertainty, the predicted states and control inputs are equivalent to the actual ones.

7 Experiments

7.1 Experimental Platform Representation

To verify the proposed predictive time-variant consensus tracking control strategy, differentially driven mobile robots are adopted as experimental plants. For the $i-th$ agent, the relationship between the control input $[v_i(t)\ \omega_i(t)]^T$ and the rotation speed of wheels $[\dot{\theta}_{il}(t)\ \dot{\theta}_{ir}(t)]^T$ is expressed as

$$
\begin{bmatrix} \dot{\theta}_{il}(t) \\ \dot{\theta}_{ir}(t) \end{bmatrix} = \frac{1}{r}\begin{bmatrix} 1 & b \\ 1 & -b \end{bmatrix}\begin{bmatrix} v_i(t) \\ \omega_i(t) \end{bmatrix} \tag{53}
$$

where r is the radius of the wheels and $2b$ is the axis length. The experimental mobile robots are driven by step motors. In the experiments, the necessary torque is less than the rated torque of step motors, therefore, the response time of step motors is ignorable. Mobile robots are located by Vicon localization system, poses of robots are transmitted from the Vicon system to each robot via User Datagram Protocol, the communication delay and packet loss between robots and the Vicon system are compensated by the networked predictive control strategy proposed in [29].

In experiments, the time synchronization is implemented on the local area network, and the inter-agent communication is achieved on the worldwide network. The inter-agent communication path is built on Aliyun cloud service. The packets from one agent to another agent is retransmitted by Aliyun servers, the networked path of inter-agent communication is illustrated in Fig.5.

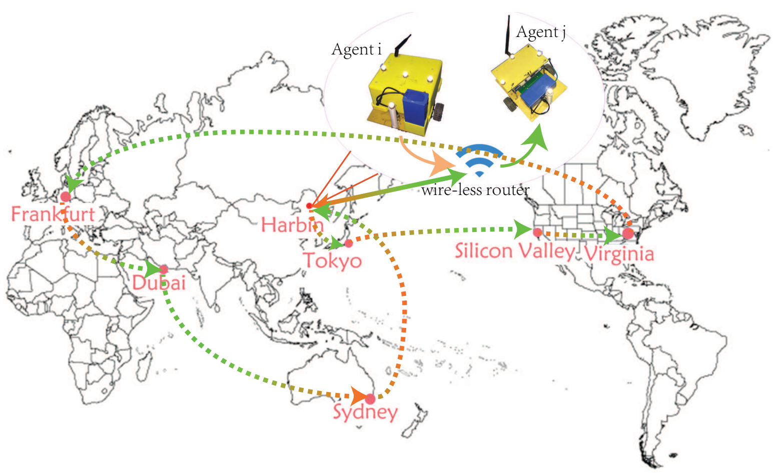

Figure 5: Networked path of packets retransmission in inter-agent communication channels

In experiments, the desired trajectory for Agent 0 to track is an eight-sharped curve expressed as

$$\begin{aligned} x(t) &= \tfrac{1.5sin(t)cos(t)}{1+\sin^2(t)} \\ y(t) &= \tfrac{1.5cos(t)}{1+\sin^2(t)} \end{aligned} \tag{54}$$

7.2 Fixed Formation with Respect to the Leader

The proposed time-variant consensus control strategy is also effective for the time-varying formation discussed in [15]. As an example, Agent 1 and Agent 2 are ordered to maintain a fixed triangle formation with respect to the body-fixed coordinate system of Agent 0. The desired positions of follower agents related to the leader agent are expressed as

$$\rho_{0i}(t) = \begin{bmatrix} \cos\varphi_0(t) & -\sin\varphi_0(t) \\ \sin\varphi_0(t) & \cos\varphi_0(t) \end{bmatrix} \begin{bmatrix} {}^0x_i \\ {}^0y_i \end{bmatrix}, i = 1, 2 \tag{55}$$

where $\left[{}^0x_i \quad {}^0y_i\right]^T$ is the desired position of Agent i with respect to Agent 0 coordinate system. The desired position of Agent 2 related to Agent 1 with respect to Agent 0 body coordinate system is expressed as

$$\rho_{12}(t) = \begin{bmatrix} \cos\varphi_0(t) & -\sin\varphi_0(t) \\ \sin\varphi_0(t) & \cos\varphi_0(t) \end{bmatrix} \begin{bmatrix} {}^0x_2 - {}^0x_1 \\ {}^0y_2 - {}^0y_1 \end{bmatrix} \tag{56}$$

In experiments, values of parameters are as follows: $\left[{}^0x_1 \quad {}^0y_1\right]^T = [-0.5 \quad -0.5]^T, \left[{}^0x_2 \quad {}^0y_2\right]^T = [-0.5 \quad 0.5]^T$. Since the desired position of followers are described with respect to Agent-0 body-fixed coordinate system, to avoid the overloaded tracking error caused by rapid rotation of Agent-0, the initial orientation of Agent-0 is nearby the tangential direction of reference trajectory. Similarly, to avoid the overloaded control gain caused by large-scale initial error, initial position of follower agents are not far from the desired one.

Fig.6 illustrates trajectories of agents; Fig.7 illustrates the tracking performance and consensus error in distance of agents in the experiment with local networked environments; Fig.8 illustrates the tracking performance and consensus error in distance of agents in the experiment with worldwide networked environments; and Fig.9 illustrates the networked delay of inter-agent communication channels in the experiment with worldwide networked environments.

The experiment results show that, under the proposed control strategy, the desired triangle formation is able to be achieved well in the worldwide networked environments as well as in the local networked environments.

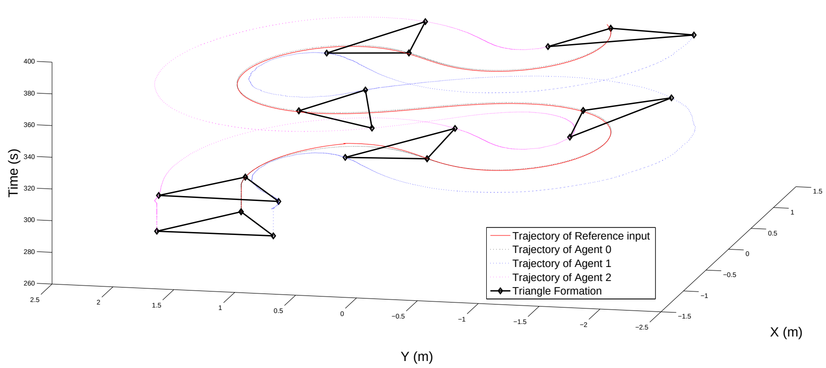

Figure 6: Trajectories of Agents in a triangle formation experiment

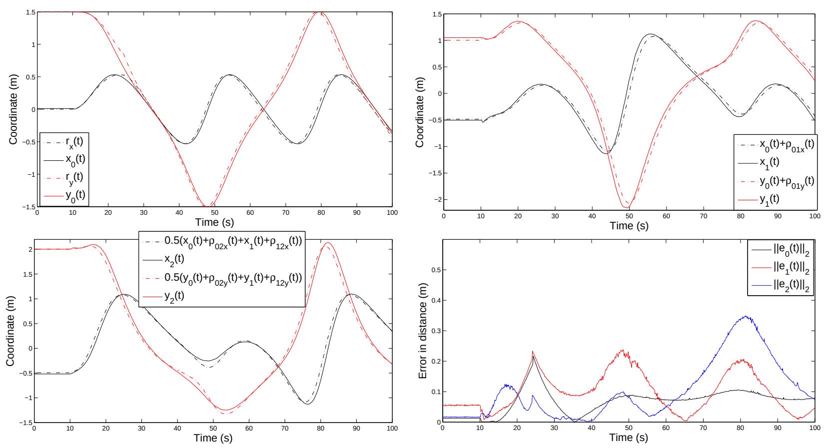

Figure 7: Tracking performance of wheeled mobile robots in the triangle formation experiment in local network

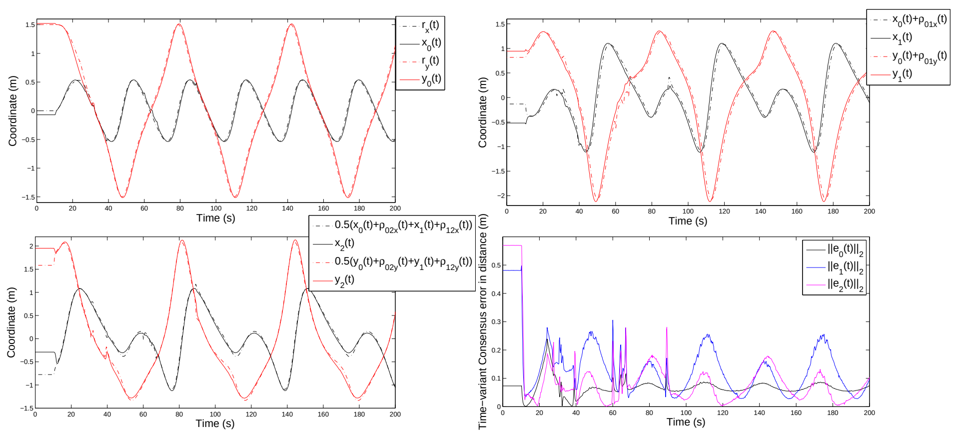

Figure 8: Tracking performance of wheeled mobile robots in the triangle formation experiment in worldwide network

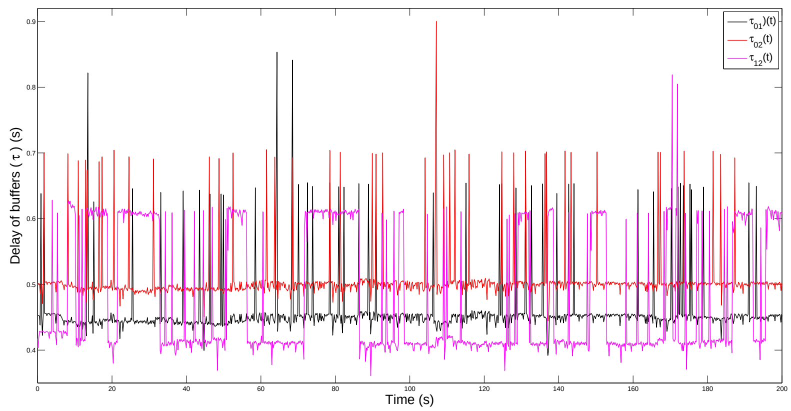

Figure 9: Communication delay of inter-agent communication in worldwide networked triangle formation experiments

7.3 Surrounding Formation

To achieve the desired time-varying formation, the converge speed of the proposed control laws is important. To verify the converge speed of the proposed control strategy, surrounding formation experiments are presented, where the leader is expected to track a desired reference trajectory and two followers are to move around the leader. Comparing with the fixed formation, the surrounding formation is more difficult, because the crash is very easy to occur as long as any agent does not track its desired position timely.

In the surrounding formation experiment, the desired positions of Agent 1 and Agent 2 related to Agent 0 with respect to the inertial coordinate system are expressed as

$$\rho_{0i}(t) = \begin{bmatrix} R_i \sin(0.3(t^*)) \\ R_i \cos(0.3(t^*)) \end{bmatrix}, t^* = \begin{cases} 0 & t \leq t_s \\ t - t_s & t > t_s \end{cases}, i = 1, 2 \tag{57}$$

where t_s is a start moment, before when all agents maintain the initial position with zero control inputs. In experiment, $R_1 = -0.75$, $R_2 = 0.75$, where position of two agents are symmetrical with respect to the position of Agent 0. Therefore, the position relationship between Agent 1 and Agent 2 is expressed as

$$\rho_{12}(t) = 2\left(\mathbf{y}_0(t) - \mathbf{y}_1(t)\right). \tag{58}$$

For easy to understand, Fig.10 illustrates a part of experimental trajectories of agents in surrounding formation experiments, where the leader tracks the reference input described as (54), simultaneously, the followers move around the leader.

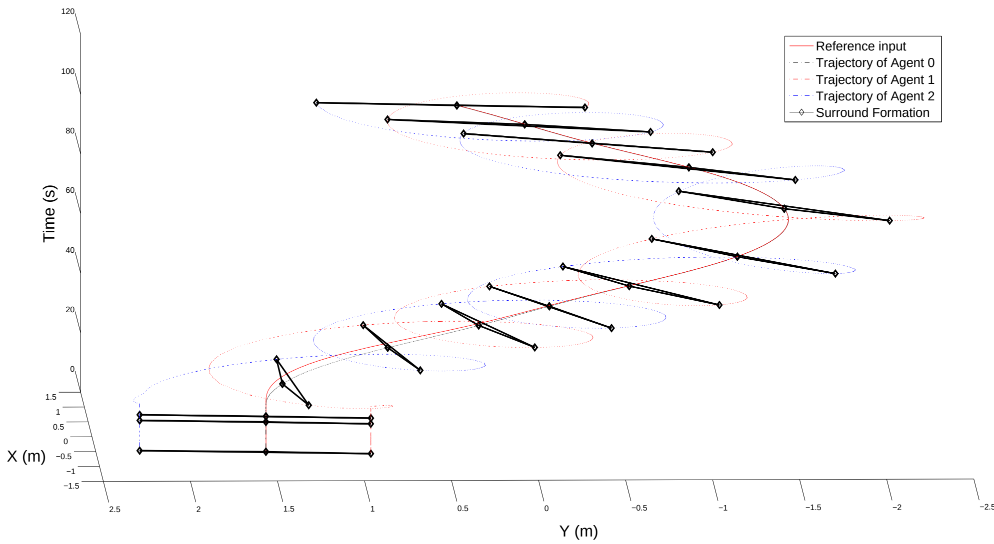

Figure 10: Trajectories of agents in a surround formation experiment

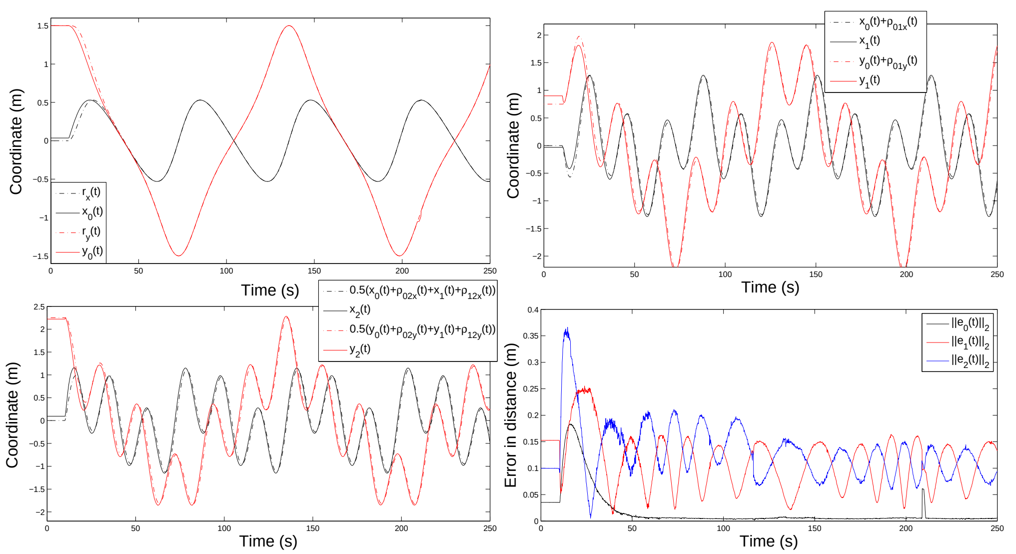

Figure 11: Tracking performance and error in distance of agents in a local networked surrounding formation experiment

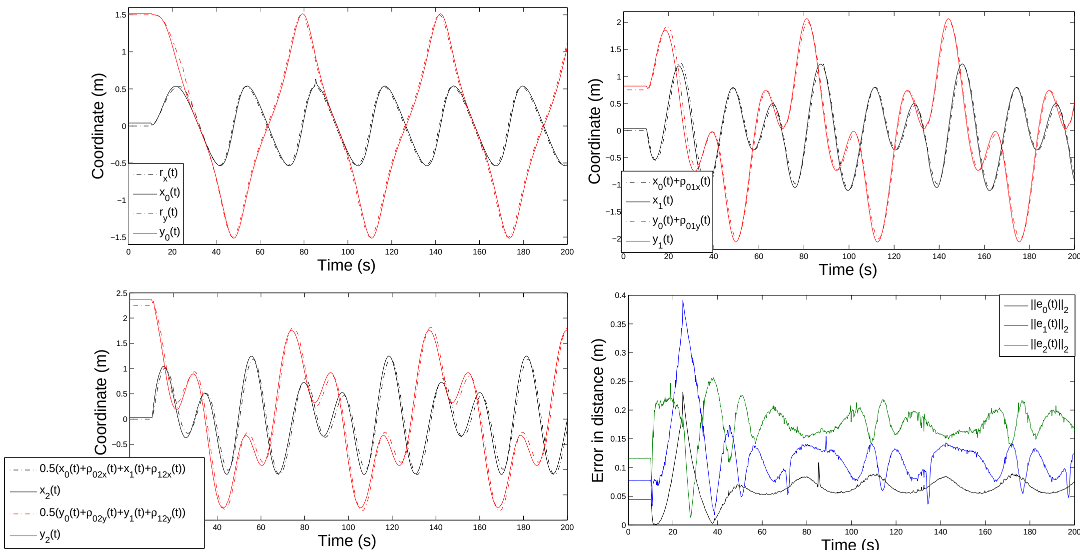

Figure 12: Tracking performace and error in distance of agent in a worldwide networked surrounding formation experiment

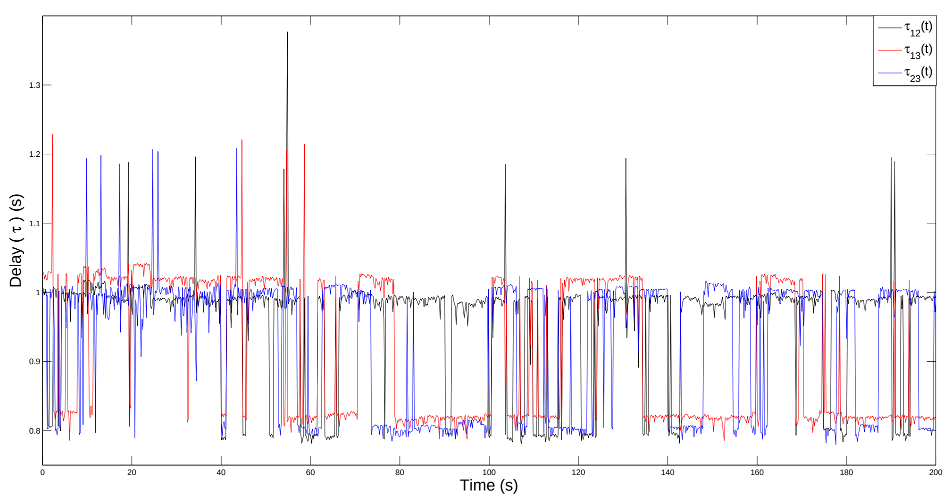

Figure 13: Communication delay of inter-agent communication in a worldwide networked surrounding formation experiment

Fig.11 illustrates the tracking performance and error in distance of agents in a surrounding formation experiment with local networked environments, Fig.12 illustrates the tracking performance and error in distance of agents in the an experiment with worldwide networked environments, and Fig.13 illustrates the communication delay between agents in the experiments with worldwide networked environments.

The experiment results show that, under the proposed control strategy, the surrounding formation is able to be achieved in the worldwide networked environments as well as in the local network. With the proposed time-variant consensus protocol, agents maintain the desired time-varying formation well. Moreover, with the proposed predictive control strategy, the communication delay of agents is compensated well, so that the proposed control strategy is effective on time-variant consensus tracking problems of non-holonomic multi-agent systems in the worldwide networked environments.

8 Conclusion

A predictive time-variant consensus tracking control strategy for planar non-holonomic multi-agent systems is presented in this article. Different from the traditional "consensus" approaches, where agents are expected to form and maintain a fixed relationship, in the time-variant consensus problem, agents are able to maintain an expected time-varying relationship as well. With the proposed time-variant consensus tracking control strategy, the leader agent is able to track the desired smooth reference input and the follower agents are able to maintain a desired time-varying formation with the leader as well. The experiment results show that, the proposed control strategy is effective for general smooth time-varying reference inputs and formations.

The other contribution of this article is the active predictive compensation scheme for multi-agent system to resist the networked delay in the inter-agent channels, where agents generate and transmit pose and control input predictions actively. Comparing with the traditional compensation mechanism for multi-agent system, where networked delay is compensated in the form of observers, in the active scheme, implementation of agents are independent and the computing efficiency of the system is improved. Moreover, the experiments are presented on the worldwide networked environments.

References

[1] Ren, W., Consensus strategies for cooperative control of vehicle formations, IET Control Theory & Applications, 2007, 1(2): 505–512

[2] Cao J, Wu Z H, Peng L., Distributed event-triggered consensus tracking of second-order multi-agent systems with a virtual leader, Chinese Physics B, 2016, 25(5): 100202.

[3] Diao M, Duan Z, Wen G., Consensus tracking of linear multi-agent systems under networked observability conditions, International Journal of Control, 2014, 87(8): 1478–1486.

[4] Chu H, Cai Y, Zhang W., Consensus tracking for multi-agent systems with directed graph via distributed adaptive protocol, Neurocomputing, 2015, 166: 8–13.

[5] Xie D, Cheng Y. Bounded consensus tracking for sampleddata secondorder multiagent systems

with fixed and Markovian switching topology[J]. International Journal of Robust and Nonlinear Control, 2015, 25(2): 252–268.

[6] Zhi-Hai W, Li P, Lin-Bo X, Stochastic bounded consensus tracking of leaderfollower multi-agent systems with measurement noises and sampled-data, Chinese Physics B, 2012, 21(12): 128902.

[7] Zhu B, Meng C, Hu G., Robust consensus tracking of doubleintegrator dynamics by bounded distributed control, International Journal of Robust and Nonlinear Control, 2016, 26(7): 1489–1511.

[8] Das B, Subudhi B, Pati B B., Cooperative formation control of autonomous underwater vehicles: An overview, International Journal of Automation and Computing, 2016, 13(3): 199–225.

[9] Yang Ao-Lei, Naeem Wasif, Fei Min-Rui, Liu Li, Multiple robots formation manoeuvring and collision avoidance strategy, International Journal of Automation and Computing, 2016, 1-10

[10] Das Bikramaditya, Subudhi Bidyadhar, Pati, Bibhuti Bhusan, Cooperative formation control of autonomous underwater vehicles: An overview, International Journal of Automation and Computing, 2016, 13(3):199-225

[11] Cruz-Morales R D, Velasco-Villa M, Castro-Linares R, Leader-follower Formation for Nonholonomic Mobile Robots: Discrete-time Approach,International Journal of Advanced Robotic Systems, 2016, 13(46)

[12] Sun D, Wang C, Shang W, et al. A synchronization approach to trajectory tracking of multiple mobile robots while maintaining time-varying formations, IEEE Transactions on Robotics, 2009, 25(5): 1074–1086.

[13] Joordens M A, Jamshidi M., Consensus control for a system of underwater swarm robots, IEEE Systems Journal, 2010, 4(1): 65–73.

[14] Yang, Zhen-Hong, Song, Yang, Zheng, Min, Hou, Wei-Yan, Consensus of multi-agent systems under switching agent dynamics and jumping network topologies, Consensus of multi-agent systems under switching agent dynamics and jumping network topologies, International Journal of Automation and Computing, 2016, 13(5):438-446

[15] Dong X, Zhou Y, Ren Z, Time-varying formation control for unmanned aerial vehicles with switching interaction topologies, Control Engineering Practice, 2016, 46: 26-36.

[16] Dong X, Han L, Li Q, Time-varying formation control for double-integrator multi-agent systems with jointly connected topologies, International Journal of Systems Science, 2015: 1–10.

[17] Dong X, Sun C, Hu G. Time-varying output formation control for linear multiagent systems with switching topologies[J]. International Journal of Robust and Nonlinear Control, 2016: 3558–3579

[18] Dong X, Hu G. Time-varying formation control for general linear multi-agent systems with switching directed topologies, Automatica, 2016, 73: 47–55.

[19] Tan C, Liu G P, Shi P., Consensus of networked multi-agent systems with diverse time-varying communication delays, Journal of the Franklin Institute, 2015, 352(7): 2934–2950.

[20] Yang X R, Liu G P., Consensus of descriptor multi-agent systems via dynamic compensators, IET Control Theory & Applications, 2014, 8(6): 389–398.

[21] Yang X R, Liu G P., Admissible consensus for networked singular multi-agent systems with communication delays, International Journal of Systems Science, 2017, 48(4): 705–714.

[22] Xiao X, Mu X., Consensus of linear multi-agent systems with communication delays by using the information of second-order neighbours under intermittent communication topology, International Journal of Systems Science, 2017, 48(1): 200–208.

[23] Han L, Dong X, Li Q, Formation-containment control for second-order multi-agent systems with

time-varying delays, Neurocomputing, 2016, 218: 439–447.

[24] Pei Y, Sun J., Consensus analysis of switching multi-agent systems with fixed topology and time-delay, Physica A: Statistical Mechanics and its Applications, 2016, 463: 437–444.

[25] Liu X, Dou L, Sun J., Consensus for networked multi-agent systems with unknown communication delays, Journal of the Franklin Institute, 2016, 353(16): 4176–4190.

[26] Yang A, Naeem W, Fei M, et al. Multiple robots formation manoeuvring and collision avoidance strategy, International Journal of Automation and Computing, 2016, 1–10

[27] Das P K, Behera H S, Jena P K, An Intelligent Multi-Robot Path Planning in a Dynamic Environment Using Improved Gravitational Search Algorithm, International Journal of Automation and Computing, 2016, 1–13

[28] Wikipedia, Breadth-first search, available on https://en.wikipedia.org/wiki/Breadth-first search, November 10, 2016

[29] Liu G P., Design and analysis of networked non-linear predictive control systems, IET Control Theory & Applications, 2015, 9(11): 1740-1745.